ANISOTROPIC MHD TURBULENCE AT LOW MAGNETIC REYNOLDS NUMBER

Anatoliy Vorobev and Oleg Zikanov
Department of Mechanical Engineering,
University of Michigan – Dearborn
Dearborn, Michigan 48128-1491, USA
vorobev@umd.umich.edu

ABSTRACT

Turbulent fluctuations in MHD flows become anisotropic under the action of a sufficiently strong magnetic field. We consider the case of low magnetic Reynolds number and investigate this phenomenon in DNS and LES simulations of forced flows in a periodic box with Re_λ up to 300 and different strengths of imposed magnetic field. Our analysis shows that both the componental (difference in amplitudes of velocity components) and dimensional (difference in velocity gradients) anisotropies are predominantly determined by the value of the magnetic interaction parameter. Degree of flow anisotropy is not significantly affected by the Reynolds number and details of large-scale forcing. It is also virtually scale-independent in a wide range of length scales.

INTRODUCTION

Magnetohydrodynamic (MHD) turbulent flows occur in numerous astrophysical, geophysical, and technological applications. In the presence of a sufficiently strong magnetic field the turbulent fluctuations become anisotropic, which implies important consequences for the properties of the turbulence and possibly requires modification of subgrid-scale closures.

A fundamentally important parameter for MHD flow is the magnetic Reynolds number,

$$Re_m \equiv \frac{uL}{\eta} \tag{1}$$

where $\eta = (\sigma\mu_0)^{-1}$ is the magnetic diffusivity, σ and μ_0 being the electric conductivity of the liquid and magnetic permeability of vacuum, and u, L are the typical velocity and length scales of the flow. The value of the parameter determines the degree to which the fluid flow perturbs the imposed magnetic field. We focus on the case of low magnetic Reynolds number, $Re_m \ll 1$. This case corresponds to a majority of technological processes. Such as continuous casting of steel and aluminum, growth of semiconductor crystals, and lithium cooling blankets for fusion reactors. At low-Re_m, the so-called quasi-static approximation can be applied (Moreau, 1990, Davidson, 2001). It can be assumed that the fluctuations of magnetic field $\mathbf{b}$ associated with fluid motions adjust instantaneously to the velocity fluctuations and that their amplitude is negligible in comparison with the amplitude of imposed magnetic field $\mathbf{B}$. The rotational part of the Lorentz force reduces to the linear functional of the velocity

$$\mathbf{F}[\mathbf{v}] = -\frac{\sigma B^2}{\rho}\triangle^{-1}\frac{\partial^2 \mathbf{v}}{\partial z^2} \tag{2}$$

where ρ and $\mathbf{u}$ are the density and velocity of the fluid, $\triangle^{-1}$ is the reciprocal Laplace operator, and we assumed that the imposed magnetic field is uniform and purely vertical $\mathbf{B} = B\mathbf{e}_z$.

The flow transformation under the impact of force (2) has been actively studied in analytical (Moffatt, 1967, Sommeria and Moreau, 1982, Davidson, 1997, Davidson, 1999), experimental (Votsish and Kolesnikov, 1976, Alemany et al., 1979) and numerical (Schumann, 1976, Zikanov and Thess, 1998, 2004) works. Far from the walls, the action of the magnetic field was identified as two-fold. First, the induced electric currents result in additional dissipation of kinetic energy, the Joule (magnetic) dissipation. Second, the flow becomes anisotropic, its structures being elongated along the magnetic field lines.

The reason for the anisotropy becomes especially transparent if one assumes that the flow is unbounded and uniform and uses the Fourier representation. The Fourier transform of (2) is

$$\widehat{\mathbf{F}}[\widehat{\mathbf{v}}] = -\frac{\sigma}{\rho}\frac{(\mathbf{B}\cdot\mathbf{k})^2}{k^2}\widehat{\mathbf{v}}(\mathbf{k},t) = -\frac{\sigma B^2}{\rho}\widehat{\mathbf{v}}(\mathbf{k},t)\cos^2\theta \tag{3}$$

where $\mathbf{k}$ is the wavenumber vector and θ is the angle between $\mathbf{k}$ and $\mathbf{B}$. The rate of Joule dissipation of a Fourier mode with the wavenumber vector $\mathbf{k}$ is

$$\mu(\mathbf{k}) = \frac{\sigma B^2}{\rho}(\widehat{\mathbf{v}}(\mathbf{k},t)\cdot\widehat{\mathbf{v}}^*(\mathbf{k},t))\cos^2\theta \tag{4}$$

so the dissipation is anisotropic. It attains maximum for the Fourier modes with $\mathbf{B} \parallel \mathbf{k}$ and zero for modes with $\mathbf{B} \perp \mathbf{k}$, i.e., for modes independent of the z-coordinate. The dissipation tends to eliminate the velocity gradients in the direction of $\mathbf{B}$ and elongate the flow structures in this direction. The limiting case is the two-dimensional state completely independent of the z-coordinate. The Joule dissipation is equal to zero in this state.

The situation looks more complicated if we take into account the non-linearity of the Navier-Stokes equations and the resulting energy transfer between the modes and tendency to restoration of isotropy. The ratio between the Lorentz force and the non-linear term of the momentum equation is evaluated by the magnetic interaction parameter (Stuart number)

$$N \equiv \frac{\sigma B^2 L}{\rho u} \tag{5}$$

It is clear that the linearized picture of the flow development discussed above is correct only in the limit of $N \gg 1$, when the inertia force is negligible in comparison with the Lorentz force. At finite N, one can expect a more complex scenario, probably with scale-dependent anisotropy.

One has to mention the possible analogy with stratified, rotating, or strained turbulence. The analogy suggests that

smaller scales are more isotropic than large scales. For example, there is a general agreement that the Kolmogorov picture of turbulent fluctuations becoming isotropic at small scales independently of the details of large-scale forcing is still valid for rotating flows since the Rossby number becomes negligible at small scales. One example is the atmospheric turbulence, completely isotropic at small-scale level.

There is no such general agreement regarding the scale dependence of anisotropy in shear flows. On the one hand, there are experimental confirmations of the Kolmogorov hypothesis (Saddoughi and Veeravalli, 1994). On the other hand, a growing number of works point out on persistent small scale anisotropy of homogeneous shear flows (Pumir and Shraiman, 1995, Biferale et al., 2004).

For the low-Re_m MHD turbulence, the question of anisotropy at different length scales has recently become particularly important in the view of attempts to apply traditional LES models (Knaepen and Moin, 2004). The comparison of the results obtained with dynamic Smagorisnky model (Germano et al., 1991) with DNS results showed good accuracy for decaying turbulence at moderate hydrodynamic Reynolds number and $N \leq 10$. This result was not totally convincing since, due to inherent limitations of DNS, the hydrodynamic Reynolds number was very moderate in the simulations. With added impact of strong Joule dissipation, the decaying flows were only weakly turbulent in the interesting case of strong magnetic field so the subgrid-scale (SGS) model was responsible only for a small fraction of the energy dissipation One can not guarantee that similarly good agreement would be obtained at higher Re. Furthermore, the conclusion of Knaepen and Moin (2004) may seem counter-intuitive since one may expect LES models developed in assumption of local isotropy to perform poorly in the case of a strongly anisotropic flow.

MODEL AND NUMERICAL EXPERIMENTS

Governing equations and forcing

We solve the equations for a forced flow of a viscous, incompressible and electrically-conducting fluid in the presence of a constant uniform vertical magnetic field $\mathbf{B} = B\mathbf{e}_z$. The quasi-static approximation is used. The Lorentz force term is given by (2). After applying $\nabla \times [\nabla \times \ldots]$ operation to eliminate pressure and taking Fourier transform, the governing equations (in dimensional form) become

$$\frac{\partial \hat{\mathbf{v}}}{\partial t}(\mathbf{k},t) = -\frac{1}{k^2}[\mathbf{k} \times (\mathbf{k} \times \hat{\mathbf{q}})] - \tag{6}$$

$$- \left[\nu \mathbf{k}^2 + \frac{\sigma B_0^2}{\rho}\left(\frac{k_z}{k}\right)^2\right]\hat{\mathbf{v}} + \widehat{\mathbf{f}}(\mathbf{k})$$

$$\mathbf{k} \cdot \hat{\mathbf{v}} = 0 \tag{7}$$

where ν is the kinematic viscosity and $\hat{\mathbf{q}}$ is the Fourier transform of the nonlinear term.

The flow is calculated within a rectangular box with periodical boundary conditions. Since we expect axial anisotropy of turbulent flow, and elongation of turbulent structures along the z-axis, the elongated box of dimensions $2\pi \times 2\pi \times 4\pi$ is used. The equation (6) is solved by the standard pseudo-spectral technique with aliasing errors fully removed by the method of phase shifting.

In order to generate a statistically steady flow over a long period of time, an artificial forcing is applied at large length scales. The external force with Fourier transform

$$\hat{\mathbf{f}}(\mathbf{k}) = \alpha(\mathbf{k})\hat{\mathbf{v}}(\mathbf{k}) \tag{8}$$

appears in (6) for Fourier modes with $1.5 \leq k \leq 3.1$. The time-dependent coefficients α are determined at each time step so that the net work by forcing is equal to the prescribed total (viscous plus magnetic) rate of dissipation ϵ_0. After a short initial development, the flow reaches an equilibrium state at which the real total dissipation rate oscillates only slightly around ϵ_0.

Two types of forcing mechanism are used. In one, the forcing is deliberately isotropic in the sense that the work is equally divided among the forced modes by chosing

$$\alpha(\mathbf{k}) = \frac{\epsilon_0}{N_{forced}(\hat{\mathbf{v}}(\mathbf{k}) \cdot \hat{\mathbf{v}}^*(\mathbf{k}))} \tag{9}$$

where N_{forced} is the number of forced modes and * stands for complex conjugate. This always keeps the forced modes three-dimensional even though they can acquire significant anisotropy due to the action of the magnetic field.

We realize that there is always a question of the impact of artificial three-dimensional forcing or, in general, behaviour of large-scale energetic modes on development of anisotropy at smaller unforced scales. To investigate the issue we perform an additional series of simulations with a purely two-dimensional forcing (referred as 'quasi 2D' in the discussion below). The same mechanism (8,9) is used but only the modes with $k_z = 0$ are forced in (8). This forcing imposes its own anisotropy at large scales.

Large-eddy simulations at higher Reynolds numbers

The method of direct numerical simulations can only be applied to flows with low to moderate Reynolds numbers. This presents an inevitable problem of insufficient scale separation between the forced and viscous dissipation subranges. One can not discern the inertial subrange of the energy spectrum.

In order to investigate the anisotropy of MHD turbulence within the inertial subrange and to reveal the effect of Reynolds number, numerical experiments at higher Re are carried out using the LES approach based on the standard dynamic Smagorinsky model (Germano et al., 1991, Lilly, 1992). In the model, the subgrid-scale force $\mathbf{f}_{sgs}$ is added to the right-hand-side of (6) in order to account for the effect of unresolved small-scale turbulent fluctuations. The force is expressed through the turbulent SGS stresses as $f_{sgs}{}_j = \partial_i \tau_{ij}$, deviatoric part of which is modeled using the eddy viscosity formula

$$\tau_{ij} - \delta_{ij}\tau_{kk} = -2C_s\Delta^2 |S| S_{ij} \tag{10}$$

where $S_{ij} = (1/2)(\partial_i u_j + \partial_j u_i)$ is the resolved rate of strain tensor, $\Delta = \sqrt[1/3]{\Delta_x \Delta_y \Delta_z}$ is the filter width based on the grid spacing in each direction, and $|S| = \sqrt{2S_{ij}S_{ji}}$. The Smagorinsky constant C_s is evaluated at each time step based on the assumption that (10) is universally valid at all inertial range length scales, which leads to

$$C_s = \frac{\langle M_{ij} L_{ji} \rangle}{\langle M_{ij} M_{ji} \rangle} \tag{11}$$

Table 1: Summary of the numerical experiments

Run	$n_x \times n_y \times n_z$	$\nu \cdot 10^3$	$Re_\lambda(t_0)$	line
(DNS)	$256 \times 256 \times 512$	2.2	94	————
(test LES)	$32 \times 32 \times 64$	2.2	91	– · – · –
(LES1)	$64 \times 64 \times 128$	2.2	93	– – – –
(LES2)	$64 \times 64 \times 128$	1.7	100	————
(LES3)	$64 \times 64 \times 128$	1	140	– – – –
(LES4)	$64 \times 64 \times 128$	0.75	170	————
(LES5)	$64 \times 64 \times 128$	0.5	200	————
(LES6)	$64 \times 64 \times 128$	0.25	290	————
(LES7)	$128 \times 128 \times 256$	0.25	290	– · · – ··
(LES-2D)	$64 \times 64 \times 128$	1	150	– · · – ··

where $\langle \ldots \rangle$ stands for spatial averaging, and tensors M_{ij} and L_{ij} are obtained as

$$L_{ij} = \hat{u}_i\hat{u}_j - \widehat{u_i u_j}, \quad M_{ij} = \hat{\Delta}^2 \left|\hat{S}\right| \hat{S}_{ij} - \Delta^2 \widehat{|S| S_{ij}} \qquad (12)$$

after application of the second sharp Fourier cut-off filtering $\hat{\ldots}$ with width $\hat{\Delta} = \sqrt[1/3]{\hat{\Delta}_x\hat{\Delta}_y\hat{\Delta}_z}$ and $\hat{\Delta}_x = 2\Delta_x$, $\hat{\Delta}_y = 2\Delta_y$, $\hat{\Delta}_z = 2\Delta_z$.

Although the applicability of traditional LES models to MHD turbulence is not obvious, we can justify the use of such a model in our study as follows. First, the Reynolds number is not very high in our simulations, so a larger fraction of viscous dissipation occurs in the resolved scales and the effect of SGS-closure should not be significant. Second, the *a-posteriori* verification by Knaepen and Moin (2004) shows that the dynamic model can be quite accurate (at least, as accurate as for ordinary non-magnetic flows) in the simulations of homogeneous MHD turbulence at moderate Re. At last, as we discuss in the concluding section of this paper, our results indicate that the dynamic model, due to its self-adjusting mechanism relying on the scale similarity within the inertial range, may be capable of adapting to anisotropic character of MHD turbulence.

Numerical experiments

Parameters of performed numerical experiments are listed in table 1. Each experiment is staged as follows (see figure 1 for an illustration). First, a developed turbulent flow is calculated starting with a random and isotropic velocity field and continuing simulations without magnetic field for a sufficiently long period. The completeness of the transitional period is judged by stabilization of the values of the total kinetic energy, viscous and magnetic dissipation rates defined as

$$E = \sum_{\mathbf{k}} E(\mathbf{k}), \quad E(\mathbf{k}) = \frac{1}{2}\left(\mathbf{v}(\mathbf{k}) \cdot \mathbf{v}^*(\mathbf{k})\right) \qquad (13)$$

$$\epsilon = \nu \sum_{\mathbf{k}} k^2 E(\mathbf{k}), \quad \mu = \frac{\sigma B_0^2}{\rho} \sum_{\mathbf{k}} \frac{k_z^2}{k^2} E(\mathbf{k}) \qquad (14)$$

At the end of this period, the DNS flow has the integral length scale $L(t_0) = 0.73$, which we evaluate as $L = \pi/(2u^2)\int_0^\infty k^{-1}E(\mathbf{k})d\mathbf{k}$, and root-mean-square velocity of turbulent fluctuations $u(t_0) = \sqrt{2/3E(t_0)} = 0.91$. Similar values are obtained in the LES experiments (see table 1).

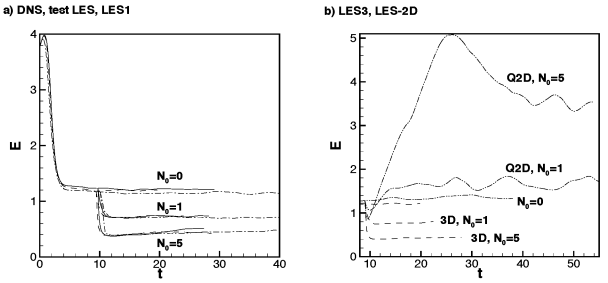

Figure 1: Evolution of total energy. *(a)* DNS (——), test LES (– · – · –) and LES1 (– – – –). *(b)* LES3 (– –) and LES-2D (– · · – · · –). For LES simulations, only the resolved part of energy is depicted. Time unit is approximately one eddy turnover time $T = L/u$ calculated for isotropic flow at $t = t_0$.

The flow field computed at the moment t_0 is used as an initial condition for three simulations with different strength of the magnetic field. For one run, the magnetic field is absent. For the other two runs corresponding to the cases of moderate and strong magnetic field, the values are chosen so that the magnetic interaction parameter (5) at this moment is $N_0 = N(t_0) \approx 1$ and $N_0 \approx 5$, respectively.

The rate of total dissipation is $\epsilon_0 = 0.5$ in all experiments, i.e., the rate of energy injection by forcing is the same for all runs. As illustrated in table 1, the difference is in the values of kinematic viscosity coefficient ν and corresponding Taylor microscale Reynolds numbers

$$Re_\lambda = \frac{u\lambda}{\nu}, \quad \lambda = \left(\frac{15\nu u^2}{\epsilon_0}\right)^{1/2} \qquad (15)$$

shown for non-magnetic flows at $t = t_0$.

The direct numerical simulations are performed with numerical resolution $256 \times 256 \times 512$ and $Re_\lambda(t_0) \approx 94$. For LES, we start with the 'test run' carried out at the same parameters as DNS but using only $32 \times 32 \times 64$ Fourier modes. The purpose of this run is to verify the accuracy of the model through direct comparison with DNS results. Further verification of the convergence of LES results is provided by LES performed at the same flow parameters as DNS and test LES but with resolution $64 \times 64 \times 128$ modes (LES1). A series of LES calculations (LES2–LES6) is performed with gradually decreasing ν in order to reveal the effect of Reynolds number. To verify the accuracy of the LES run corresponding to the largest Reynolds number, $Re_\lambda \approx 290$, as well as to examine convergence of LES simulations, an additional run (LES7) is performed at the same parameters as LES6 but with resolution of $128 \times 128 \times 256$ modes. Finally, to investigate the influence of the large-scale forcing on the flow characteristics, the run (LES-2D) with quasi-2D forcing and all other parameters identical to (LES3) is performed.

Flow evolution

The evolution of total energy is shown in figure 1. Time is measured in dimensional units in all figures. Using the values of L and u in developed isotropic flow at $t = t_0$, we can evaluate the typical eddy turnover time as $T(t_0) \approx 1$. It can be seen that the periods of initial flow development and adjustment after the introduction of magnetic field last several turnover times, after which the flow becomes statistically steady. In the

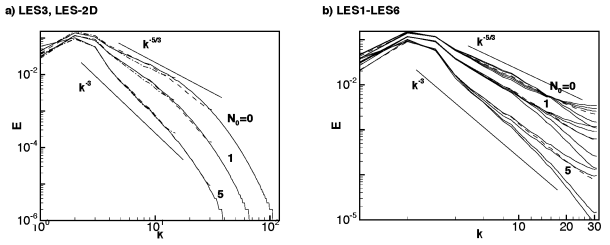

Figure 2: Spectra of kinetic energy. *(a)* DNS (——), test LES (– · – · –) and LES1 (– – – –). *(b)* LES1-LES6

flows with magnetic field, the Joule dissipation is responsible for a major part of the total dissipation rate.

The energy curves for DNS, test LES (figure 1a) and LES1–LES6 are almost identical, which is expectable since this global quantity is dominated by large-scale modes of the flow governed by identical forcing in these experiments. On the contrary, the behaviour of energy in LES-2D experiment with two-dimensional forcing (figure 1b) is completely different. It is obviously dominated by slow evolution of large-scale quasi-two-dimensional structures. Similar results were obtained for the time evolution of rates of viscous and magnetic dissipation (not shown here).

The spectra of energy and viscous and magnetic dissipation rates were obtained for the equilibrium stages of each experiment. Several velocity fields separated by, at least, one turn-over time were used for averaging. One can see in figure 2a that the spectra obtained in DNS, test LES and LES1 are very close. This can be considered as an indication of the accuracy of the dynamic LES model.

The spectra for non-magnetic runs at higher Reynolds number (see figure 2b) show clear scale separation with about a decade of $k^{-5/3}$ scaling. The high-k ends are affected by the SGS modeling, especially in the runs with largest Re_λ, which have typical upward facing tails. In the presence of the magnetic field, the energy spectra become steeper approaching k^{-3} slope at $N_0 = 5$.

The internal structure of the flow is illustrated in figure 3, where we plot snapshots of modified pressure field Π_1 made in developed flows at different magnetic fields and different forcing. The pressure field is calculated using the Poisson equation,

$$\nabla^2 \Pi_1 = \rho \nabla \cdot [\mathbf{v} \times \mathbf{w}] \qquad (16)$$

Here $\mathbf{w} = \nabla \times \mathbf{v}$ is vorticity, and we assume $\rho = 1$.

Figures 3a,b demonstrate that there are no noticeable differences between the visual structures of flows obtained in DNS and LES. The tendency to developing anisotropy under the action of imposed magnetic field is clearly seen, although even at $N_0 = 5$ the flow is far from approaching purely two-dimensional form. On the contrary, the snapshots of modified pressure in the flows with quasi 2D forcing in figure 3c show almost 2D structures for the run with strong magnetic field and high degree of anisotropy for moderate and non-magnetic runs. This clearly demonstrates the dominating role played by the largest scale modes in determining the visible patterns often demonstrated in the literature.

ANISOTROPY

Generally, one has to distinguish between two types of anisotropy, componental and dimensional. Componental

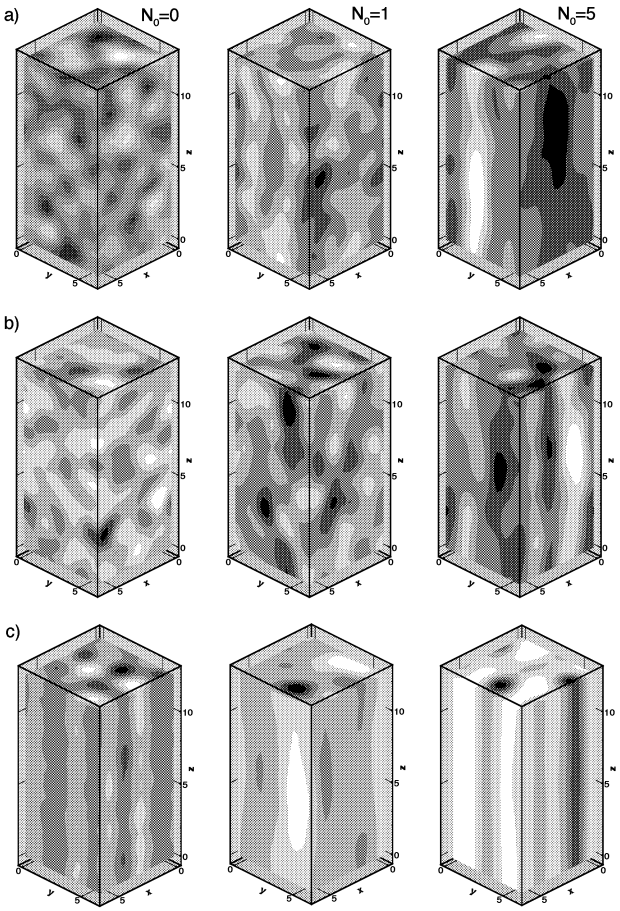

Figure 3: Modified pressure fields in developed flows. *(a)* DNS, *(b)* test LES, *(c)* LES-2D

anisotropy is understood as anisotropy of the Reynolds stress tensor or, in other words, inequality between the components of the velocity field (Kassinos et al., 2001). Dimensional anisotropy characterizes the difference in derivatives of a function taken along different directions (anisotropy of gradients). The Joule dissipation directly affects only the velocity gradients along the magnetic field lines, i.e., dimensional anisotropy. The componental anisotropy is a secondary effect, whose existence, strength, and relation to the intensity of the magnetic field are far from being obvious.

Anisotropy at different length scales

We now approach the main question of our paper, that of dependence of the anisotropy properties of MHD turbulence on the length scale. A closely related question stems from the fact that, as demonstrated in our simulations, the integral anisotropy characteristics are affected by details of large-scale forcing, i.e., by flow-specific behaviour of energy containing modes. It is not clear how strong is this effect for small-scale turbulent fluctuations and whether there is a range of scales, where anisotropy possesses 'universal' properties unaltered by the large-scale dynamics.

We start with the dimensional anisotropy. The first indications that it can be scale-independent were obtained in DNS of Zikanov and Thess (1998). It was found, that the steepen-

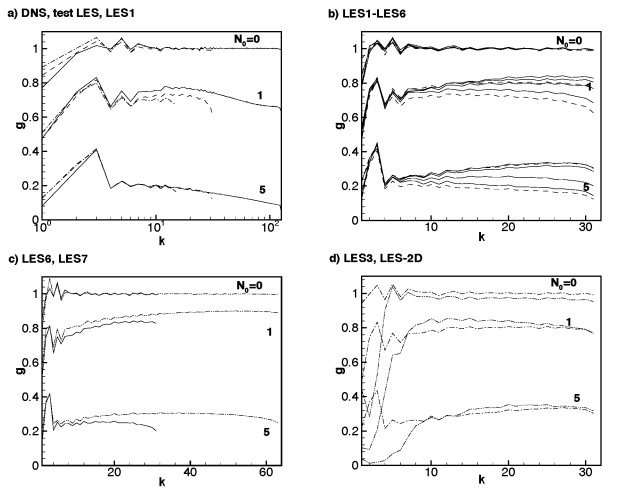

Figure 4: Spectra of anisotropy coefficient (17). *(a)* DNS (——), test LES (– · – · –) and LES1 (– – – –). *(b)* LES1-LES6. *(c)* LES6 (———) and LES7 (– · · – · · –). *(d)* LES3 (– – –) and LES-2D (– · · – · · –)

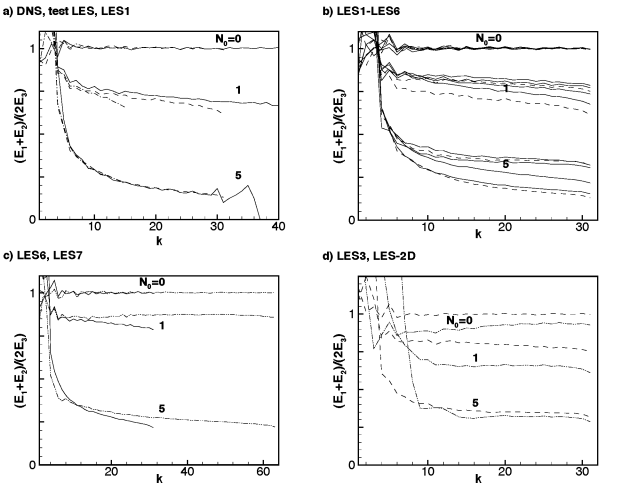

Figure 5: Spectra of the ratio $(E_1 + E_2)/2E_3$, componental anisotropy coefficient. *(a)* DNS (——), test LES (– · – · –) and LES1 (– – – –). *(b)* LES1-LES6. *(c)* LES6 (———) and LES7 (– · · – · · –). *(d)* LES3 (– – –) and LES-2D (– · · – · · –)

ing of the energy spectrum with growing N is closely followed by the steepening of the Joule dissipation spectrum. This behaviour is confirmed in our simulations for larger Reynolds numbers and different forcing. The ratio

$$g(k) \equiv \frac{3\tau}{2}\frac{\mu(k)}{E(k)} = \frac{3\sum \frac{k_z^2}{k^2}\hat{\mathbf{u}}\cdot\hat{\mathbf{u}}^*}{\sum \hat{\mathbf{u}}\cdot\hat{\mathbf{u}}^*} = \frac{3D_{33}(k)}{2E(k)} \qquad (17)$$

can be considered as a measure of dimensional anisotropy at the wavelength k. In (17), the sums are over all wavenumber vectors in the shell $k - 1/2 < |\mathbf{k}| \le k + 1/2$ and D_{33} is the component of the dimensionality tensor considered by Kassinos et al. (2001). The scaling factor is chosen so as to provide $g = 1$ in an isotropic flow. In a purely two-dimensional flow with zero magnetic dissipation, $g(k) \equiv 0$.

One can see that there is a good agreement between the results of DNS and test LES in figure 4a. Together with similar agreement observed for componental anisotropy (see figure 5a) this serves as another confirmation of accuracy of the LES model.

Important conclusions can be deduced from figure 4. Most importantly, in all experiments, there is a significant range of length scales, where the dimensional anisotropy coefficient varies only slightly with k. The range starts almost immediately outside the forced region and extends to the smallest resolved length scales. This behaviour was observed in all our numerical experiments including DNS and LES with three-dimensional and two-dimensional forcing. In some LES runs, $g(k)$ seems to vary faster with k at small length scales when k approaches the cut-off. This is an artefact caused by imperfection of SGS model. We repeated the LES6 run with four times smaller cut-off scale (LES7). As one can see in figure 4c, shifting the LES filter to smaller scales results in corresponding extension of the range where the anisotropy is scale-independent.

It can also be seen that the anisotropy in this range is almost solely determined by the strength of the magnetic field. Some effect of the Reynolds number is present, with $g(k)$ having tendency to increase slightly with Re. This effect, however, is much weaker than the effect of the magnetic interaction parameter. Another interesting fact is fast disappearance of the sensitivity to forcing seen in figure 4d. The 2D forcing explicitly introduces the dimensional anisotropy into the large scales. Within the forced region, $g(k)$ for LES-2D run is about two times smaller than for the corresponding 3D forcing run LES3. When, however, k leaves the region, the two curves converge quickly and become close for all three values of N_0. The visually different flows obtained with isotropic and two-dimensional forcing (cf., figures 3a,b and 3c) possess, at the same strength of the magnetic field, similar degrees of anisotropy of small-scale turbulent fluctuations.

To analyze the componental anisotropy we calculate the ratio of typical parallel and perpendicular velocity components at different length scales. Figure 5 shows

$$c(k) = \frac{E_1(k) + E_2(k)}{2E_3(k)} \qquad (18)$$

where

$$E_i(k) = \frac{1}{2}\sum_{k-1/2<|\mathbf{k}|<k+1/2} \left(v_i(\mathbf{k})\cdot v_i^*(\mathbf{k})\right), \qquad i = 1,2,3 \qquad (19)$$

Scale-dependence of componental anisotropy can be described in terms similar to those used above for dimensional anisotropy. We see in figure 5 that, outside of the forced region of the spectrum, the coefficient $c(k)$ varies only slightly with k for all values of N. As in the case of dimensional anisotropy, the scale-independence was consistently observed in all our experiments. Comparison between DNS curves in figure 5a and curves for LES6 and LES7 in figure 5c shows that the extension of the scale range of the flow leads to corresponding extension of the subrange, where the anisotropy is constant.

As shown in figure 5b, the Reynolds number does not seriously affect the componental anisotropy. It is interesting to see in figure 5d that the anisotropy of energy containing scales does not cascade down the spectrum or otherwise noticeably affects the smaller scales. Even though there is some difference between LES and LES-2D curves in figure 5d, especially

at $N_0 = 0$ and $N_0 = 1$, the strength of the magnetic field still remains the dominant factor determining the value of $c(k)$ at non-forced scales.

CONCLUSIONS

- In the presence of a sufficiently strong magnetic field, the flow develops dimensional and componental anisotropies
- Both types of anisotropy only slightly depend on the length-scale outside the range of large-scale energy containing modes, where the forcing is performed
- Our simulations do not show any variations in the degree of flow anisotropy at length scales approaching the smallest resolved scales of the flow. We can not, however, exclude the possibility that different behaviour can be observed at much higher Reynolds numbers. On the other hand, the extent of the range of constant anisotropy was found to be quite significant in our simulations (about 2 orders of magnitude). The scale-invariance seems to be a persistent feature of low-Re_m MHD turbulence
- Both types of anisotropy are only slightly affected by the Reynolds number
- Dimensional and componental anisotropies caused by forcing are essential only at the length scales close to the forced scales. At smaller scales, the effect of the large-scale dynamics on turbulent fluctuations quickly subsides.

To summarize, our simulations clearly demonstrate that the anisotropy of low-Re_m MHD turbulence at length scales outside the energy-containing range is a robust function of the magnetic interaction parameter unaffected by the scale, hydrodynamic Reynolds number, and details of the large-scale dynamics.

The work also confirms that dynamic Smagorinsky eddy-viscosity model provides a good approach to simulations of anisotropic MHD turbulent flows. Indeed, a-posteriori verification of the model using comparison between DNS and test LES runs has consistently shown a good agreement for flow characteristics such as the spectra of energy, viscous and magnetic dissipation, and the anisotropy of resolved scales.

In fact, in view of our conclusion about scale-invariance of anisotropy, good performance of the dynamic model is not at all surprising. In the model, we determine the coefficient C_s based on the assumption that (10) holds universally within a certain scale range, so the same coefficient C_s can be applied at grid and test filter widths. If the anisotropy is scale-independent, the MHD correction to (10), whatever it may be, is the same for both filters so the adjustment mechanism should work with the same accuracy as in the non-magnetic isotropic case.

An extended version of this paper is currently being prepared for submission to the Journal of Fluid Mechanics. Part of this work was performed during the 2004 Summer Program at the Center for Turbulence Research with financial support from Stanford University and NASA Ames Research Center. The authors would like to thank P. Moin and N. Mansour for their hospitality during the stay. The authors have benefited from numerous fruitful discussions with A. Thess, P.A. Davidson, B. Knaepen, R. Moreau, S. Kassinos, and D. Carati.

The work was supported by the grant DE FG02 03 ER46062 from the US Department of Energy. The computations were performed on the NASA Ames and NERSC (Department of Energy) parallel computers and on the parallel computer cluster at the University of Michigan - Dearborn acquired with the support of the grant CTS 0320621 from the MRI program of the National Science Foundation.

REFERENCES

Alemany, A., Moreau, R., Sulem, P. L., and Frisch, U., 1979, "Influence of external magnetic field on homogeneous MHD turbulence", *J. de Mecanique*, 18, 280–313.

Biferale, L., Daumont, I., Lanotte, A., and Toschi, F., 2004, "Theoretical and numerical study of highly anisotropic turbulent flows", *European Journal of Mechanics B/Fluids*, 23, 401–414.

Davidson, P. A., 1997, "The role of angular momentum in the magnetic damping of turbulence", *J. Fluid Mech.*, 336, 123–150.

Davidson, P. A., 1999, "Magnetohydrodynamics in Materials Processing", *Annu. Rev. Fluid Mech.*, 31, 273–300.

Davidson, P. A., 2001, "An Introduction to Magnetohydrodynamics", Cambridge University Press, Cambridge.

Germano, M., Piomelli, U., Moin, P., and Cabot, W. H., 1991, "A dynamic subgrid-scale eddy viscosity model", *Phys. Fluids A*, 3, 1760–1765.

Kassinos, S. C., Reynolds, W. C., and Rogers, M. M., 2001, "One-point turbulence structure tensors", *J. Fluid Mech.*, 428, 213–248.

Knaepen, B., and Moin, P., 2004, "Large-eddy simulation of conductive flows at low magnetic Reynolds number", *Phys. Fluids*, 16, 1255–1261.

Lilly, D. K., 1992, "A proposed modification to the Germano subgridscale closure model", *Phys. Fluids A*, 4, 633–635.

Moffatt, H. K., 1967, "On the suppression of turbulence by a uniform magnetic field", *J. Fluid Mech.*, 28, 571–592.

Moreau, R., 1990, "Magnetohydrodynamics", Kluwer Academic Publishers, Dordrecht.

Pumir, A., and Shraiman, B. I., 1995, "Persistent small scale anisotropy in homogeneous shear flows", *Phys. Rev. Letters*, v. 75, N. 17, 3114–3117.

Saddoughi, S. G., and Veeravalli, S. V., 1994, "Local isotropy in turbulent boundary layers at high Reynolds number", *J. Fluid Mech.*, 268, 333–372.

Schumann, U., 1976, "Numerical simulation of the transition from three- to two-dimensional turbulence under a uniform magnetic field", *J. Fluid Mech.*, 74, 31–58.

Sommeria, J., and Moreau, R., 1982, "Why, how, and when, MHD turbulence becomes two-dimensional", *J. Fluid Mech.*, 118, 507–518.

Votsish, A. D., and Kolesnikov, Yu. B., 1976, "Investigation of transition from three-dimensional turbulence to two-dimensional under a magnetic field", *Magn. Hydrodyn.*, 3, 141-142.

Zikanov, O., and Thess, A., 1998, "Direct numerical simulation of forced MHD turbulence at low magnetic Reynolds number", *J. Fluid Mech.*, 358, 299–333.

Zikanov, O., and Thess, A., 2004, "Direct numerical simulation as a tool for understanding MHD liquid metal turbulence", *Appl. Math. Mod.*, 28, 1–13.